



Variation of the characteristics of biofilm on the semi-suspended bio-carrier produced by a 3D printing technique: Investigation of a whole growing cycle



Bing Tang*, Yiliang Zhao, Liying Bin, Shaosong Huang, Fenglian Fu

School of Environmental Science and Engineering and Institute of Environmental Health and Pollution Control, Guangdong University of Technology, 510006 Guangzhou, PR China

ARTICLE INFO

Keywords:

Micro-habitat
Biofilm
3D printing technique
Semi-suspended bio-carrier
Microbial community

ABSTRACT

The presented investigation focused on exploring the characteristics of the biofilm formed on a novel semi-suspended bio-carrier and revealing their variation during the whole growing cycle. This used semi-suspended bio-carrier was designed to be a spindle shape, and then fabricated by using a 3D printing technique. Results indicated the bio-carrier provided a suitable environment for the attachment of diverse microorganisms. During the experimental period lasted for 45 days, the biofilm quickly attached on the surface of the bio-carrier and grew to maturity, but its characteristics, including the chemical compositions, adhesion force, surface roughness, structure of microbial communities, varied continuously along with the operational time, which greatly influenced the performance of the bioreactor. The shape and structure of bio-carrier, and the shearing force caused by the aeration are important factors that influence the microbial community and its structure, and also heavily affect the formation and growth of biofilm.

1. Introduction

Biofilm is a kind of well self-balanced microbial aggregates that attaches on the surface of bio-carriers, in which, lots of microorganisms compose a microbial community with a clear function, and generally act as a main body to degrade organic pollutants and convert nutrients in both natural or artificial bio-processes (Karunakaran et al., 2011). Comparing with a conventional activated sludge (CAS) process, biofilm can provide a safer habitat for the contained microbial community to resist the damage of surrounding environment (Ivnitsky et al., 2007), and more importantly, the attached status is also very suitable for the growth of slow growing microorganisms (Chen et al., 2016), which is of vital importance for the biological conversion of nutrients. Obviously, the excellent performance of a biofilm reactor totally depends on the formation of sufficient and stable biofilm within a bio-reactor, and one of the essential factors to determine the formation and the characteristics of biofilm is the properties of bio-carrier (or bio-packing) (Masłóń & Tomaszek, 2015; Tang et al., 2017b). Because of which not only provides a suitable space for the microbial community to grow on, but also determines the distribution of air and water flowing within the bioreactor. The former is a crucial factor to construct a habitat for the survival of microbial species, and the latter dominates the mass transferring within the reactor, which heavily influences the supplying of oxygen, substrates and nutrients, and the removal of metabolites.

Commonly used bio-carriers include the fixed bio-carriers and the suspended bio-carriers, the former refers to the conventional bio-packing that is installed fixedly in a bioreactor, and the latter is the kind of bio-carriers that can move freely in a bioreactor. The fixed bio-carriers must be properly installed in a bioreactor before its operation, and can be homogeneously packed, which generally achieve a higher filling ratio. However, when the biofilm grows too thick and fully fills the packing, two major defects, including low efficiency of mass transferring and clogging of the bioreactor, gradually become dominant and are quite difficult to overcome. The suspended bio-carriers need not to be installed in advance, and they can be packed in a bioreactor with a certain volume ratio, which compose a so-called moving bed bioreactor (MBBR). When an MBBR is filled with water, the packed bio-carriers are totally suspended under the action of flowing water and air, and can move freely in the bioreactor, which greatly improve the mass transferring within the bioreactor. However, due to the shearing force caused by the flowing water and air, and the friction among bio-carriers, the successful formation of biofilm on bio-carriers is quite a slow and difficult process, which greatly postpones the start-up of bioreactors (Mao et al., 2017). To a large extent, the type of bio-carrier may influence the formation and structure of biofilm, and further determines the operation of a bioreactor (Felföldi et al., 2015; Lackner et al., 2009), therefore, a new kind of bio-carrier with high-performance is extremely needed for enhancing the performance of biofilm reactors (Deng et al.,

* Corresponding author at: No. 100, Waihuan Xi Road, Guangzhou Higher Education Mega Center, Guangzhou 510006, PR China.
E-mail addresses: renytang@163.com, tang@gdut.edu.cn (B. Tang).

2016).

Considering both the advantages and disadvantages of the conventional fixed and suspended bio-carriers, a logic approach is to design a new kind of bio-carrier that combines the advantages of the conventional bio-carriers. Based on such an idea, a semi-suspended bio-carrier with spindle-shape was designed. Nevertheless, such a complex structure is quite difficult to be fabricated with a regular molding method. With the development of material-molding technology, the three-dimensional (3D) printing technique develops very rapidly and is gradually becoming mature, which is capable of fulfilling the task of making very complex shapes and structures in an accurate way. In recent years, 3D printing techniques have been used in the fields of human tissue engineering (Brunello et al., 2016), drug production (Norman et al., 2017), and even the fabrication of feed spacer in membrane systems for water treatment (Siddiqui et al., 2016), which exhibit a promising prospect that can never be imagined before. Therefore, with this novel technique, the semi-suspended bio-carrier was designed and fabricated for the first time (Tang et al., 2017a).

As an aggregation of numerous microorganisms, the biofilm has its own growing cycle on a bio-carrier, which includes the following stages: the attachment of bacteria on the surface, colonization, maturation, aging and detachment. Each stage shows special characteristics, which heavily influences the performance of the relevant bioreactor (Mao et al., 2017). In this regard, the variation of biofilm during its growing cycle should be the primary consideration in investigating and designing this new type of bio-carrier. So far, the published literature mainly reported the characteristics of biofilm on traditional bio-carriers and only focused on the mature stage, and there is still no enough knowledge available for fully understanding the variation of biofilm during its whole growing cycle, especially on the surface of a semi-suspended bio-carrier. Obviously, such an issue is an obstacle to the accurate design and operation management of the bioreactor that packs with these new bio-carriers. Many factors influence the variation of biofilm during its entire growing cycle, including the nutrients, the temperature, the characteristics of bio-carrier, the pH values and the hydrodynamic conditions within the bioreactor (Capua et al., 2017; Prades et al., 2017). However, the shape and structure may play important roles in the operation of a biofilm reactor. On one hand, they provide a necessary habitat for the microbial organisms to attach on. On the other hand, it is an essential factor to determine the distribution of water and air flowing, and further influence the mass transfer of dissolved oxygen (DO) and nutrients. Formation of a mature biofilm is no doubt an important factor to determine the successful operation of a biofilm reactor, but the shearing force (generally caused by the aerated air) detaches the biofilm from the surface of bio-carrier, which decreases the bioactivity of biofilm. Thus, the combined effects of the bio-carrier and the shearing force caused by aeration should be an essential factor to be considered. For this purpose, this work mainly focused on investigating the variation of the characteristics of biofilm on a semi-suspended bio-carrier fabricated by using a 3D printing technique. Considering the combined effects of the shape and structure of the bio-carrier and the shearing force on the biofilm formation during the operation period, two closely related aspects were studied, which included: (1) designing a novel semi-suspended bio-carrier with a spindle-shape and fabricating it with a 3D printing technique; (2) comparing the variation of the characteristics of biofilm on the bio-carrier during its whole growing cycle under two different aeration rates. It's hoped the results would provide useful references to the development of this new kind of bio-carrier.

2. Materials and methods

2.1. Basic parameters of the semi-suspended bio-carrier

Even on the same bio-carrier, the biofilms at different positions are subject to different shearing forces, which may have an obvious

influence on the growth of biofilm. The bio-carrier was designed to be a spindle shape with evenly distributed tiny holes on the surface, whose detailed design drawing was shown in Supporting Information (SI) and the structural parameters were listed in a previous investigation (Tang et al., 2017a). After having finished the design, a 3D printing technique was used to fabricate the bio-carrier with the mixture of isocyanate (PX 118-ISOCYANATE) and polyhydric alcohols (PX118-FPOLYOL and PX118-L POLYOL) to be the moulding material. For making a comparison, two different positions (Cell 1 and Cell 2, SI) on the bio-carrier were chosen to evaluate their effects on the growth of biofilm.

2.2. Bioreactor configuration and the experimental process

The used experimental apparatus was a self-designed bioreactor with rectangular shape, whose working volume was 100 L (60 × 50 × 40.8 cm), and it was divided equally into two zones by a baffle and used to conduct all the experiments. Two aerators were installed separately at the bottom of each zone. One zone, aerated in the rate of 0.3 L/min air, was labeled as the “A” zone, and the other zone, aerated in the rate of 3.0 L/min air, was labeled as the “B” zone. Two same metal frames, supported by a holder, were installed above the two aerators. The schematic diagram of the experimental system is shown in SI.

The inoculated sludge was collected from the secondary sedimentation tank of a local wastewater treatment plant (WWTP) (Lijiao municipal wastewater treatment plant, located at Haizhu District, Guangzhou, China). The initial inoculation concentration was controlled at about 1500 mg/L mixed liquid suspended solids (MLSS, 0.15% TSS), and the filling ratio of bio-carriers was set at 30% in the bioreactor. The influent was the synthetic wastewater prepared by mixing tap water with the concentrated nutrient solution containing various kinds of nutritive salts (C₆H₁₂O₆ 6H₂O: 233.3 mg/L; NH₄Cl: 69.1 mg/L; C₄H₇NaO₄: 100 mg/L; KH₂PO₄: 15.9 mg/L; NaHCO₃: 65 mg/L; MgSO₄: 40.4 mg/L; MnSO₄: 13.57 mg/L; CaCl₂: 31.25 mg/L; FeSO₄: 1.1 mg/L) with the ratio of COD:N:P at 100:5:1. Other operational conditions include: hydrodynamic retention time (HRT): 24 h; flux: 0.09 L/min.

2.3. Evaluation of the performance of the bioreactor

Regular water quality indexes, including COD, NH₃-N, NO₂⁻-N, NO₃⁻-N, and total nitrogen (TN), were selected to evaluate the performance of the bioreactor, and were measured according to the standard method (APHA et al., 2005). NH₃-N, NO₂⁻-N, NO₃⁻-N was measured separately, while, TN was calculated on the basis of the sum of NH₃-N, NO₂⁻-N, NO₃⁻-N rather than independent tests. Two DO probes (JPSJ-605F, INESA, China) were installed in the middle of both the “A” and “B” zones, respectively, and they were connected directly to a computer to record the DO value of the corresponding zones. In the mentioned two zones, the DO values were measured simultaneously every 10 s and stored in a connected computer during the whole operational period, and then the final DO values were calculated on their averaged value per minute according to the data obtained from the computer. With the different aeration rates in the “A” (0.3 L/min) and “B” (3 L/min) zones, the influence of aeration rate on the growth of biofilm could be investigated. The values of pH were measured by a pH meter (pH2-S, INESA, China).

2.4. Morphology observation and roughness measurement of the biofilm surface

The adhesion force between the biofilm and the surface of bio-carriers was measured by using an atomic force microscope (AFM) (Dimension Fastscan, Bruker Inc., Germany), the images and force-distance curves of the biofilm were measured and scanned in a contact mode using silicon nitride cantilever with a spring constant of 0.13 N/m

at a speed of 1.0 Hz with 256 by 256 resolutions.

The surface roughness of biofilm was obtained by analyzing the observed images by AFM with the attached software of NanoScope. The root-mean-square average roughness (R_q , nm) were used to quantitatively evaluate the surface roughness of the biofilm at different growing stage (Tang et al., 2016).

2.5. Extraction and analysis of extracellular polymeric substance (EPS)

EPS is the substance secreted by microorganisms in their metabolism, which is generally responsible for aggregating free microorganisms together to form a stable aggregates. In a biofilm system, the compositions of EPS are very complex and have a close relationship with the stability of biofilm. In the experiment, the composition of EPS and their variation over time were evaluated by their content at different positions in the bioreactor. At a pre-set time interval, the biofilm was stripped from the surface on bio-carrier in distilled water, and then, the tightly bound EPS (TB-EPS) and loosely bound EPS (LB-EPS) were extracted from the obtained biofilm by referencing the method of a reported literature (Li & Yang, 2007). Both the TB-EPS and LB-EPS were analyzed for the contained protein (PN) and polysaccharide (PS). The concentration of PN was determined by the modified Lowry method (Frolund et al., 1995) using bovine serum albumin (BSA) (BR, Sino-pharm Chemical Reagent Co., Ltd, China) as the standard. The PS concentration was determined with the anthrone-sulfuric acid method (Raunkjær et al., 1994) using glucose (AR, Tianjin Damao Chemical Reagent Factory, China) as the standard. And the correlation between the adhesion force and the EPS in biofilm was analyzed by the software of IBM SPSS 20.0.

2.6. Analysis of the composition of the microbial community on the bio-carrier

To evaluate the variation of the microbial community of biofilm at the different positions during the whole growing cycle, the biofilm samples were collected at the selected positions of the bio-carriers at pre-set time points. The biofilm samples for analyzing the microbial community were taken from both Cell 1 and Cell 2 on the surface at different operational stages (the 30th and 40th day), which represented for the microbial community at the stages of maturity and detachment, respectively. These samples were labeled as, MUA, MDA, MUB, MDB, DUA, DUB, DUA and DDA, each sample was marked with the name shown in Table 1. For making a comparison, the inoculated sludge was also taken as a sample, which was labeled as “I”.

The determination of the species and microbial community in these samples were all performed by an HTS method including the processes of DNA extraction and PCR amplification of 16S rRNA gene. After finishing these processes, the obtained PCR products were sent for

Table 1
The details of the biofilm samples for AFM and biodiversity measurement.

Sample's name	Growing stage	Sampling time	Position in the bio-carrier	Zone in the reactor
MUA	Attachment	Day 6	Cell 1	A
MUB				B
MDA			Cell 2	A
MDB				B
DUA	Maturity	Day 30	Cell 1	A
DUB				B
DDA			Cell 2	A
ddb				B
IUA	Detachment	Day 40	Cell 1	A
IUB				B
IDA			Cell 2	A
IDB				B

sequencing by using the Hiseq platform (Hiseq, IlluminaInc, USA). Depending on the regional characteristics of amplification 16S and the products of double terminal sequencing (Paired-End) obtained by Illumina HiSeq sequencing platform, the method of building a small fragment library with double terminal sequencing was used, with which, the sample species could be revealed by splicing and filtering the Reads, clustering of the Operational Taxonomic Units (OTUs), and analyzing of the annotation and the abundance of species. Additionally, further analysis of the Alpha diversity and the Beta Diversity could reveal the differences among the samples.

3. Results and discussion

3.1. Variation of DO value in the bioreactor

The performance of an aerobic bioreactor is influenced by the concentration of DO, in which, the DO value is not only influenced by the aeration rate, but also by the packed bio-carrier. To test the performance of this new bio-carrier under different aeration rates, the special configuration of the bioreactor was built up, whose DO distribution in the two zones during the whole experimental period is shown in Fig. 1.

Due to a 10-fold difference in the aeration rate, the actual DO values in the “A” and “B” zone show quite an obvious difference even they have the same configuration and bio-carrier filling ratio. However, along with the operational time, the DO value in both the zones gradually decreases, which indicates more oxygen was consumed by the growing microorganisms in the bioreactor. At the initial stage (from day 1 to 15), in the “A” zone, the DO value was at relatively low values (less than 2.0 mg/L), and decreased very quickly to no more than 1.0 mg/L. From the 26th day till to the end of the experiment, the DO concentration kept under 0.4 mg/L; in the “B” zone, with a relatively lower initial inoculated concentration of MLSS, the DO value was 6.76 mg/L on the first day of the experiment, which indicated DO consumption was not very high. However, shortly after the start-up, DO value declined very quickly, and on the 15th day, the DO value was around 3–4 mg/L, and after the 26th day, the DO value reached at a stable value (around 2.5 mg/L) till the end of the experiment. The stable DO values of the latter stage in both “A” and “B” zone indicated that the supplying and consumption of oxygen finally reached a balance as the growth of microorganisms in the bioreactor.

3.2. Surface roughness measurement and morphology observation of the biofilm

The bioreactor was operated continuously under the operational conditions (listed in Section 2) for 45 days. At pre-set time intervals, the bio-carriers were taken out to measure the surface roughness of the attached biofilm with an AFM. For making a comparison, the samples were collected from both the “A” and “B” zones in the bioreactor. The samples for roughness measurement of Cell 1 and Cell 2 in the bio-carriers from the “A” and “B” zones were marked as UA, DA, UB and

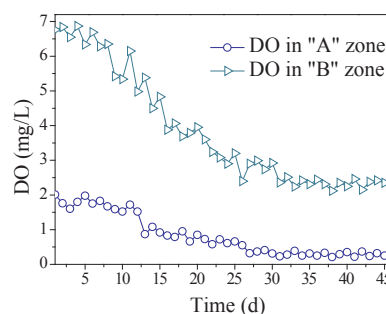


Fig. 1. Variation of the DO value over time in the two zones of the bioreactor.

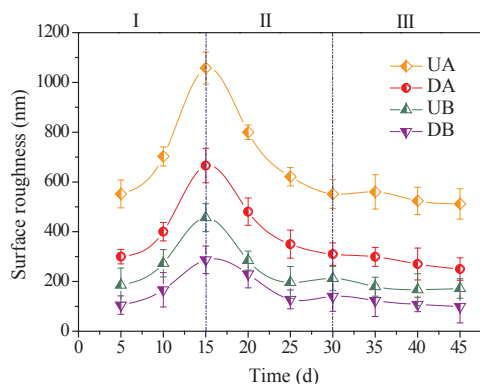


Fig. 2. Surface roughness of the biofilm.

DB, respectively. The results are shown in Fig. 2.

After start-up, the surface roughness of the formed biofilm was measured every 5 days till the last day. As shown in Fig. 2, the surface roughness of biofilm exhibits a similar tendency in the varying pattern at the different positions of the bio-carrier and different zones of the bioreactor during the growing cycle. However, the values of surface roughness of biofilm are quite different along with the positions in the bioreactor. In general, the biofilm in the “B” zone has a lower value in the surface roughness than that of in the “A” zone, and at the position on Cell 1, it also exhibits a higher value of surface roughness than that at the position on Cell 2. Comparing with the “A” and “B” zones, the most dominant difference is the aeration rate. A larger aeration rate in the “B” zone means a higher shearing force imposing on the surface of biofilm, which is beneficial to reduce the surface roughness of biofilm. In addition, the spindle-shape also results in an obvious difference in the shearing force on the surface at the position of Cell 1 and Cell 2 even on a single bio-carrier. The above results indicate that the shearing force has a dominant influence on the surface roughness of biofilm. For further illustrating the phenomenon, the biofilm samples were collected on the given positions of the bio-carriers at a different operational time, and their 3D AFM images are shown in Fig. 3.

The 3D AFM images in Fig. 3 give a visual description of the distribution of peak and valley on the biofilm surface with different colors (Tang et al., 2016), in which, a yellow color stands for a peak on the biofilm surface, and a lighter color means a higher peak, while, a brown color stands for a valley on the surface, and a darker color means a deeper valley. Fig. 3(a)–(d) show the morphology of newly formed biofilm, which exhibit lots of rugged peaks. In this period, dispersed microorganisms attached on the surface of the bio-carriers, and gradually formed an integrated biofilm. However, for the formed biofilm did not totally cover all the area, only peaks were presented on the surface. As the growth of biofilm to the maturity stage, more microorganisms attached on the surface and the dispersed microbial aggregates combined to form an integrated biofilm, which greatly reduced the difference between the peaks and the valleys. Fig. 3(e)–(h) reveal the morphology of biofilm in the maturity stage, which show less peaks presenting on the surface than that in the attachment stage. As the biofilm was aging, they gradually detached from the surface, Fig. 3(i)–(l) exhibit more valleys presenting on the surface than that of the former two stages. The results in Fig. 3 indicate that the biofilm at all stages and all positions on the bio-carrier have the same growing cycle and varying tendency.

3.3. Adhesive force between the biofilm and the surface of bio-carrier

The adhesive force between the biofilm and the surface of bio-carrier reflects the physical stability of the biofilm, which is an important factor to determine the performance of a bio-process. For fully understanding its variation, the adhesive force was measured every 6 days

after the bioreactor being started, and the results are shown in Fig. 4.

Adhesive force is a quantitative parameter to describe the physical strength of biofilm, which is influenced by many factors. The results in Fig. 4 show the adhesive force increases to a peak value and then decreases to a flat level, which exhibit a similar tendency in the varying trend of the surface roughness on the bio-carrier. Comparing the actual values of the obtained data, the biofilms in the “B” zone at both of the sampling positions (Cell 1 and Cell 2) have higher values in the adhesive force than that in the “A” zone at the corresponding positions, which indicates that, even on the same bio-carrier, the biofilm attached on the larger end (Cell 2) also has a strong adhesive force than that on the smaller end (Cell 1). In the “B” zone, nearly ten times aeration rate is provided than that in the “A” zone, which produces a greater shearing force and strips the loose biofilm on the surface. Such a shearing force causes the remained biofilm possessing higher mechanical stability, which exhibits larger values in the adhesive force. In this meaning, the shearing force is an essential factor influencing the mechanical strength of the biofilm on the bio-carrier, and further affects the composition of biofilm.

3.4. Variation of EPS over time in the biofilm at different positions

EPS is also an essential factor to influence the stability of biofilm. However, the composition of EPS is quite complex and totally dependent on the operational conditions in an actual bioreactor. In general, bound EPS is directly responsible for the stability of biofilm, and can be roughly classified as LB-EPS and TB-EPS, and among them, PN and PS may account for more than a 85% ratio (Baroutian et al., 2013), which determine the basic characteristic of biofilm to a large extent. For fully understanding the variation of each kind of EPS over time, the biofilm samples were collected at a pre-set time interval from the different zones and positions in the used bioreactor during the whole growing cycle. The results are shown in Fig. 5.

EPS mainly includes PN and PS, and in TB-EPS and LB-EPS, they are labeled as TB-PN, TB-PS, LB-PN and LB-PS, respectively. At the positions of Cell 1 and Cell 2, the corresponding numbers are marked subsequently in Fig. 5. The main role of the bound EPS in biofilm is to keep the microorganisms together. However, along with the operation of the bioreactor, the content of each kind of EPS at different zones of the bioreactor and the positions on bio-carrier may change to different degrees.

Comparing with the total contents of EPS in both the “A” and “B” zones, a rather similar profile in the varying trend of total EPS can be observed, which indicates the changing pattern of EPS in these two zones is quite consistent. At the “B” zone, a ten-fold aeration rate is provided, which causes a relatively larger shearing force on the surface of the bio-carrier to detach the biofilm than that at the “A” zone, and as a result, it shows an obviously higher content of each kind of EPS at any positions in the “B” zone than that in the “A” zone.

The values of LB-EPS and TB-EPS in the “B” zone are higher than that in the “A” zone, which confirms that a higher aeration rate is beneficial to the stability of biofilm. Due to the increasing of EPS secreted by microorganisms under a higher aeration rate, larger cohesiveness in biofilm may generally present (Pellicier-Nacher & Smets, 2014). TB-EPS, showing the best flocculation capability, generally increases easier than other EPS at a higher aeration rate, whose attachment on the surface of bio-carriers is dependent on the properties of the water within the bioreactor (especially the pH value) (Pellicier-Nacher & Smets, 2014; Zhang et al., 2014). Interestingly, the contents of TB-EPS in Cell 2 are 68.34 mg/gVSS (B) and 33.51 mg/gVSS (A), respectively, which are close to that in Cell 1 (61.48 mg/gVSS (B) and 29.57 mg/gVSS (A)) on the 25th day. While, the value of LB-EPS shows an obvious difference at the “B” zone between Cell 1 (31.13 mg/gVSS (B)) and Cell 2 (49.34 mg/gVSS (B)). On the used bio-carrier, Cell 2 has a relative a larger volume and higher depth, and can hold more biomass within it, which may be the reason to explain why the value of EPS is

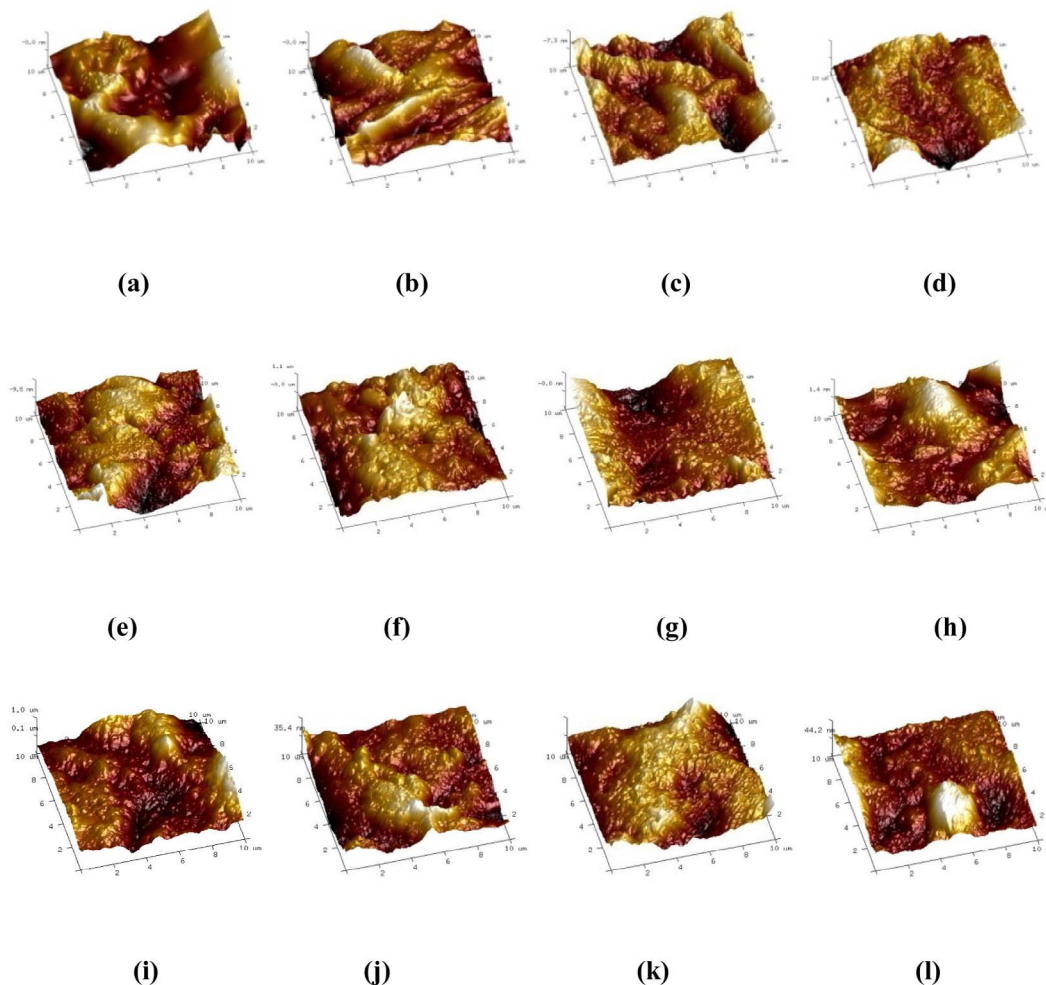


Fig. 3. 3D structure of the morphology of biofilm on the bio-carrier at different times: (a)–(l) represents the samples of MUA, MDA, MUB, MDB, DUA, DDA, DUB, DDB, IUA, IDA, IUB, IDB, respectively.

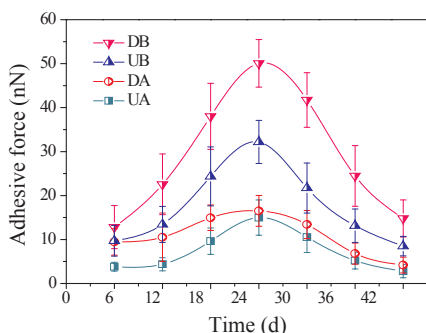


Fig. 4. Variation of the adhesive force during the growing cycle.

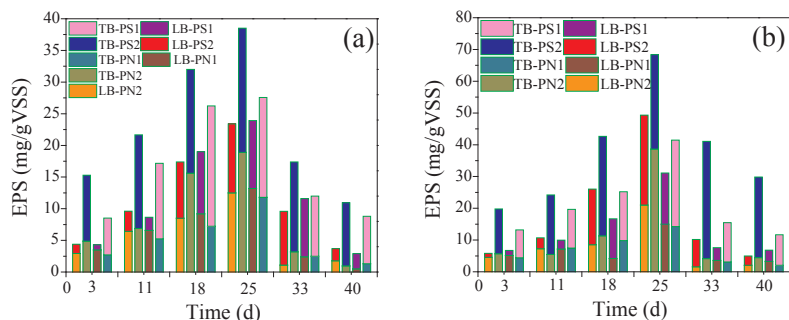


Fig. 5. Variation of EPS in the biofilm at different zones and positions (1, 2 mean the samples from Cell 1 and Cell 2, respectively): (a) varying trend of the EPS in the biofilm of “A” zone; (b) varying trend of the EPS in the biofilm of “B” zone.

Table 2
Correlation between the adhesion force and the EPS in biofilm of both zones.

		LB-PN2	TB-PN2	LB-PS2	TB-PS2	LB-PN1	TB-PN1	LB-PS1	TB-PS1
Zone A	r	0.724	0.845 ^c	0.951 ^{***}	0.925 ^{***}	0.676	0.743	0.942 ^{***}	0.635
	P	0.104	0.034	0.003	0.008	0.141	0.091	0.005	0.175
Zone B	r	0.586	0.681	0.874 ^a	0.863 ^a	0.633	0.766	0.922 ^{***}	0.909 ^a
	P	0.222	0.136	0.023	0.027	0.177	0.076	0.009	0.012

Where r is the Pearson correlation, P is the significance of correlation.

^{***} At 0.01 level (2-tailed) significance correlation.

^a At 0.05 level (2-tailed) significance correlation.

3.5. Analysis of the microbial biodiversity of the biofilm

For illustrating the structure of microbial communities in the biofilm and verifying the biodiversity of the bioreactor, the samples from the inoculated sludge and the positions on bio-carrier at the stages including the attachment and maturity (Table 1) were collected, and the distribution of microorganisms inside the biofilm at different positions was analyzed by using an HTS method. The results are shown in Fig. 6.

"I" is the sample of inoculated sludge, which stands for the original microbial community. In Fig. 6(a) and (b), the results reveal the similarity and difference in the numbers of OTUs among all samples. At the attachment stage (Fig. 6(a), only 6 days after start-up), the shared OTUs among the five samples are 667, and the unique OTUs among them are 230 (I), 75 (MUA), 76 (MDA), 104 (MUB), and 93 (MDB), respectively. The shared OTUs account for the largest ratio, but the numbers of unique OTU also indicate the species at the different positions of bio-carrier appears a differentiation, while, at the maturity stage (Fig. 6(b), operating for 30 days), the shared OTUs are 583, and the unique OTUs are 277 (I), 139 (DUA), 154 (DDA), 111 (DUB), and 93 (DDB), respectively. Comparing these two stages, the number of shared OTUs decreases from 667 to 583, and the total number of the unique OTUs increases from 578 to 774, which indicates the biodiversity of microbial community improving from the initial start-up to the maturity stage.

After the floated microbes attach on the surface of bio-carriers, they colonize to form a biofilm and gradually establish microbial communities with a clear function, which totally determine the performance of bioreactor. For further illustrating the biodiversity of microbial community in the biofilm, the results of HTS were exhibited in the forms of the relative abundance at class level, the heat map at the genus level, and the principal coordinate analysis (PCoA). The results are shown in Fig. 6(c) and (d).

Microorganisms are important components in bioreactors. However, not a single species of microorganism can determine the successful operation of the bioreactor, but a whole microbial ecosystem, composed by numerous microorganisms and their surrounding conditions, plays an actual role in degrading organic pollutants and converting nutrients (Demeter et al., 2017). In this regards, only the whole microbial community contained in the biofilm is responsible for the performance of a biofilm reactor. As shown in Fig. 6(c), the microbial community developed in the attachment stage is mainly composed of *Proteobacteria* (MUA: 77.3%, MDA: 76.5%, MUB: 64.8%, MDB: 69.9%), and some *Bacteroidetes* (MUA: 14.8%, MDA: 13.6%, MUB: 25.2%, and MDB: 17.1%), while, the relative abundances of *Firmicute* (MUA: 2.1%, MDA: 2.6%, MUB: 3.4% and MDB: 5.9%, respectively), *Actinobacteria* (MUA: 1.4%, MDA: 2.2%, MUB: 1.2 and MDB: 1.9%, respectively) and *Chloroflexi* (MUA: 0.5%, MDA: 0.4%, MUB: 0.2 and MDB: 0.4%, respectively) are relative lower. Meanwhile, at the class level, the samples of MUA, MDA, MUB and MDB developed in the attachment stage are dominated by *Gama-Proteobacteria* (28.3%, 27.8%, 14.6%, and 19.1%, respectively), *Beta-Betaproteobacteria* (26.1%, 27.7%, 28.7%, and 21.5%, respectively), *Alpha-Proteobacteria* (17.2%, 15.8%, 12.8%, and 22.6%, respectively), but *Delta-Proteobacteria* is found to be less than 10%. The main strains of *Proteobacteria* are *Enterobacteriales* (11.6%, 11.7%, 4.6%, and 8.9%, respectively) and *Rhodocyclales* (13.7%,

10.6%, 15.5% and 10.4%, respectively), they belong to the family of *Enterobacteriaceae* and *Rhodocyclaceae*. While *Beta-Proteobacteria* is mainly consisted of the strains *Burkholderiales* (10.3%, 14.9%, 11.5% and 9.1%, respectively) and is dominated by the family of *Comamonadaceae*.

However, in the samples of DUA, DDA, DUB, DDB, the dominated bacteria are *Gamma-Proteobacteria* (21.1%, 15.7%, 17.7%, and 23.6%, respectively), *Beta-Proteobacteria* (18.6%, 14.5%, 20.6% and 22.4%, respectively), *Alpha-Proteobacteria* (12.3%, 7.1%, 14.3% and 12.4%, respectively) and *Delta-Proteobacteria* (10.9%, 13.9%, 5.4% and 7.1%, respectively). The main strains of *Proteobacteria* are *Enterobacteriales* (3.5%, 3.2%, 1.5% and 0.6%, respectively), *Rhodocyclales* (8.8%, 7.5%, 8.1% and 8.2%, respectively), and *Burkholderiales* (7.2%, 4.7%, 10.1% and 12.1%, respectively).

As shown in Fig. 6(c), in the inoculated sludge, *Gamma-Proteobacteria* (35.1%), *Alpha-Proteobacteria* (16.3%), *Beta-Proteobacteria* (9.9%), *Sphingobacteria* (4.5%) are the dominant groups. However, it is interesting to find that the ratios of *Gamma-Proteobacteria*, *Beta-Proteobacteria*, and *Alpha-Proteobacteria* in the biofilm seem to decrease from the attachment to the maturity stage despite the increasing level of *Delta-Proteobacteria*. The high abundance of *Gamma-Proteobacteria* confirms that the biofilm is a potential reservoir of this kind of microorganism (Douterelo et al., 2013), which implies that the detached biofilm may decrease the abundance of *Gamma-Proteobacteria* biofilm. Moreover, *Beta-Proteobacteria* are comprised of organic matter decomposing bacteria, ammonia oxidizing bacteria (AOB), nitrite oxidizing bacteria (NOB), and denitrifying bacteria, who can attach more easily onto the surface of bio-carriers and dominate the process of biofilm formation in freshwater ecosystems (Douterelo et al., 2013; Hoang et al., 2014). In addition, *Alpha-Proteobacteria* is found ubiquitously in activated sludge, wastewater, and sediments, which plays a main role to degrade various organic contaminants. The lower abundance of *Alpha-Proteobacteria* and higher abundance of *Beta-Proteobacteria* in the biofilms may reflect higher biofilm stability under a medium shearing force (Ivnitsky et al., 2007). *Bacillus* strains, belonging to the phylum of *Firmicutes*, display the impressive physiological diversity of resisting high temperature and highly acidic condition as well as inducing both the removal of volatile fatty acids and denitrification in a system where there is a process of simultaneous aerobic nitrification/denitrification (Al Ashhab et al., 2014; Zhou et al., 2015). Nevertheless, Class *Sphingobacteria*, belonging to the phylum of *Bacteroidetes*, has an important role in the hydrolysis of complex organic molecules (Prachanurak et al., 2014).

The genus level is shown in Fig. 6(d), which indicates that the main genus within *Gama-Proteobacteria* in the sample I, MUA, MDA, MUO, MDO, DUA, DDA, DUO, DDO are *Zoogloea* (0.5%, 8.6%, 5.9%, 9.1%, 6.1%, 1.6%, 1.5%, 2.8% and 3.6%, respectively), and most of the *Zoogloea* members belong to the family *Rhodocyclaceae*, while *Flavobacteriia* mainly consists of the *Flavobacterium* genus (0.5%, 1.8%, 2.4%, 5.6%, 3.4%, 0.9%, 0.8%, 0.9% and 3.9%, respectively) dominated by the *Flavobacteriaceae* family. Additionally, *Bacilli* is dominated by the genus *Lactococcus* belonging to the *Streptococcaceae* family. Generally, *Flavobacterium* can degrade a wide range of macromolecules (such as proteins and carbohydrates), and also plays a main role in

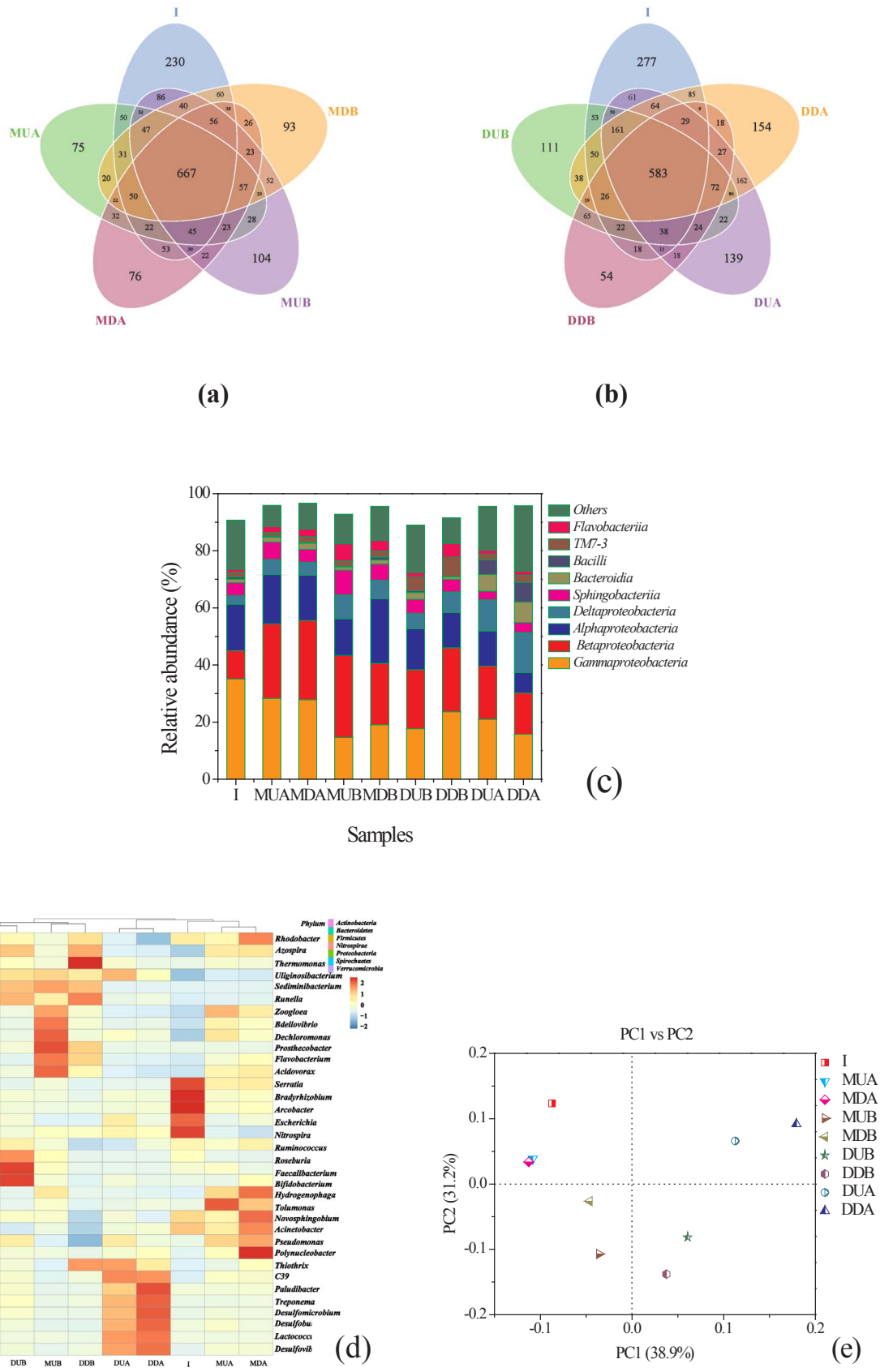


Fig. 6. Analysis of the biodiversity on the bio-carriers: (a) the OTU numbers at the attached stage; (b) the OTU numbers at the maturity stage; (c) relative abundance at the class level; (d) heat map at the genus level; (e) PCoA based on the weighted unfract distance.

denitrification (Islam et al., 2014). Some of *Bacteroidetes* can enhance the removal of biological phosphorus (Al Ashhab et al., 2014), while, *Zoogloea bacteria*, a kind of well-known filamentous bulking microorganisms in CAS facilities, can form large assemblages and secrete stronger EPS than other microbes, and is abundant under oligotrophic conditions (Douterelo et al., 2013; Young et al., 2016; Zhu et al., 2015). Additionally, *Lactococcus* can produce interconnected quinones with a membrane-shape structure to transfer electrons to the electrochemically active Gram-positive bacteria as an acceptor of extracellular electrons (Zhou et al., 2015).

The result of PCoA based on the weighted unifractal distance is shown in Fig. 6(e), which indicates a continuous succession of the microbial community from the primary to the mature biofilm. The inoculated sludge represents the original community the bioreactor. However, the used bio-carrier has a novel structure, which causes a significant difference in the biofilm thickness, and forms an obvious micro-profile of DO value to create multi micro-habitats on the semi-suspended bio-carrier (Tang et al., 2017a). Their great influence on the succession of the microbial community has brought an obvious difference in the composition of microbial communities between the biofilm in the two cells of bio-carrier. The above results demonstrate that the microbial community at different position of biofilm exhibits quite different composition, which further verifies the shape and structure of bio-carriers are important factors to heavily influence the microbial community.

4. Conclusions

A semi-suspended bio-carrier with a spindle shape was fabricated by a 3D printing technique and used in this work, which exhibited a special effect on the characteristics of the attached biofilm during its whole growing cycle. The results indicated that the shape and structure of the bio-carrier, and the shearing force caused by the aeration were important factors that influenced the microbial community and its succession, and also heavily affected the formation and growth of biofilm, which were verified to be very essential to forming multi micro-habitats in a single bioreactor and promoting the biodiversity within the bioreactor.

Acknowledgements

This work was supported by the National Natural Science Foundation of China [Grant number of 21476050]; and the Foundation of High-level Talents of Guangdong Province [Grant Number 20140009].

Appendix A. Supplementary data

Supplementary data associated with this article can be found, in the online version, at <http://dx.doi.org/10.1016/j.biortech.2017.07.132>.

References

Al Ashhab, A., Gillor, O., Herzberg, M., 2014. Biofouling of reverse-osmosis membranes under different shear rates during tertiary wastewater desalination: microbial community composition. *Water Res.* 67, 86–95.

APHA, AWWA, WPCF, 2005. Standard Methods for the Examination of Water and Wastewater, 21st ed. American Public Health Association, Washington, DC.

Baroutian, S., Eshtiaghi, N., Gapes, D.J., 2013. Rheology of a primary and secondary sewage sludge mixture: dependency on temperature and solid concentration. *Bioresour. Technol.* 140, 227–233.

Brunello, G., Sivoletta, S., Meneghello, R., Ferroni, L., Gardin, C., Piattelli, A., Zavan, B., Bressan, E., 2016. Powder-based 3D printing for bone tissue engineering. *Biotechnol. Adv.* 34 (5), 740–753.

Capua, F.D., Lakaniemi, A.-M., Puhakka, J.A., Lens, P.N.L., Esposito, G., 2017. High-rate thiosulfate-driven denitrification at pH lower than 5 in fluidized-bed reactor. *Chem. Eng. J.* 310, 282–291.

Celmer, D., Oleszkiewicz, J.A., Cicek, N., 2008. Impact of shear force on the biofilm

structure and performance of a membrane biofilm reactor for tertiary hydrogen-driven denitrification of municipal wastewater. *Water Res.* 42 (12), 3057–3065.

Chen, F., Bi, X., Ng, H.Y., 2016. Effects of bio-carriers on membrane fouling mitigation in moving bed membrane bioreactor. *J. Membr. Sci.* 499, 134–142.

Demeter, M.A., Lemire, J.A., Mercer, S.M., Turner, R.J., 2017. Screening selectively harnessed environmental microbial communities for biodegradation of polycyclic aromatic hydrocarbons in moving bed biofilm reactors. *Bioresour. Technol.* 228, 116–124.

Deng, L., Guo, W., Ngo, H.H., Zhang, X., Wang, X.C., Zhang, Q., Chen, R., 2016. New functional biocarriers for enhancing the performance of a hybrid moving bed biofilm reactor-membrane bioreactor system. *Bioresour. Technol.* 208, 87–93.

Douterelo, I., Sharpe, R.L., Boxall, J.B., 2013. Influence of hydraulic regimes on bacterial community structure and composition in an experimental drinking water distribution system. *Water Res.* 47 (2), 503–516.

Felföldi, T., Jurecska, L., Vajna, B., Barkács, K., Makk, J., Cebe, G., Szabó, A., Zárny, G., Márialigeti, K., 2015. Texture and type of polymer fiber carrier determine bacterial colonization and biofilm properties in wastewater treatment. *Chem. Eng. J.* 264, 824–834.

Frolund, B., Griebe, T., Nielsen, P.H., 1995. Enzymatic activity in the activated-sludge floc matrix. *Appl. Microbiol. Biotechnol.* 43 (4), 755–761.

Hoang, V., Delatolla, R., Abujamel, T., Mottawea, W., Gadbois, A., Laflamme, E., Stintzi, A., 2014. Nitrifying moving bed biofilm reactor (MBBR) biofilm and biomass response to long term exposure to 1 degrees C. *Water Res.* 49, 215–224.

Islam, M.S., Dong, T., Sheng, Z., Zhang, Y., Liu, Y., Gamal El-Din, M., 2014. Microbial community structure and operational performance of a fluidized bed biofilm reactor treating oil sands process-affected water. *Int. Biodeterior. Biodegrad.* 91, 111–118.

Ivnitsky, H., Katz, I., Minz, D., Volvovic, G., Shimoni, E., Kesselman, E., Semiat, R., Dosoretz, C.G., 2007. Bacterial community composition and structure of biofilms developing on nanofiltration membranes applied to wastewater treatment. *Water Res.* 41 (17), 3924–3935.

Karunakaran, E., Mukherjee, J., Ramalingam, B., Biggs, C.A., 2011. “Biofilmology”: a multidisciplinary review of the study of microbial biofilms. *Appl. Microbiol. Biotechnol.* 90 (6), 1869–1881.

Lackner, S., Holmberg, M., Terada, A., Kingshott, P., Smets, B.F., 2009. Enhancing the formation and shear resistance of nitrifying biofilms on membranes by surface modification. *Water Res.* 43 (14), 3469–3478.

Li, X.Y., Yang, S.F., 2007. Influence of loosely bound extracellular polymeric substances (EPS) on the flocculation, sedimentation and dewaterability of activated sludge. *Water Res.* 41 (5), 1022–1030.

Mao, Y., Quan, X., Zhao, H., Zhang, Y., Chen, S., Liu, T., Quan, W., 2017. Accelerated startup of moving bed biofilm process with novel electrophilic suspended biofilm carriers. *Chem. Eng. J.* 315, 364–372.

Masloń, A., Tomaszek, J.A., 2015. A study on the use of the BioBall® as a biofilm carrier in a sequencing batch reactor. *Bioresour. Technol.* 196, 577–585.

Norman, J., Madurawe, R.D., Moore, C.M., Khan, M.A., Khairuzzaman, A., 2017. A new chapter in pharmaceutical manufacturing: 3D-printed drug products. *Adv. Drug Delivery Rev.* 108, 39–50.

Pellicier-Nacher, C., Smets, B.F., 2014. Structure, composition, and strength of nitrifying membrane-aerated biofilms. *Water Res.* 57, 151–161.

Prachanurak, P., Chiemchaisri, C., Chiemchaisri, W., Yamamoto, K., 2014. Biomass production from fermented starch wastewater in photo-bioreactor with internal overflow recirculation. *Bioresour. Technol.* 165, 129–136.

Prades, L., Dorado, A.D., Climent, J., Guimera, X., Chiva, S., Gamisans, X., 2017. CFD modeling of a fixed-bed biofilm reactor coupling hydrodynamics and biokinetics. *Chem. Eng. J.* 313, 680–692.

Raunkjær, K., Hvitved-Jacobsen, T., Nielsen, P.H., 1994. Measurement of pools of protein, carbohydrate and lipid in domestic wastewater. *Water Res.* 28 (2), 251–262.

Siddiqui, A., Farhat, N., Bucs, S.S., Linares, R.V., Picioreanu, C., Kruthof, J.C., van Loosdrecht, M.C.M., Kidwell, J., Vrouwenvelder, J.S., 2016. Development and characterization of 3D-printed feed spacers for spiral wound membrane systems. *Water Res.* 91, 55–67.

Tang, B., Song, H.L., Bin, L.Y., Huang, S.S., Zhang, W.X., Fu, F.L., Zhao, Y.L., Chen, Q.Y., 2017a. Determination of the profile of DO and its mass transferring coefficient in a biofilm reactor packed with semi-suspended bio-carriers. *Bioresour. Technol.* 241, 54–62.

Tang, B., Yu, C.F., Bin, L.Y., Zhao, Y.L., Feng, X.F., Huang, S.S., Fu, F.L., Ding, J.W., Chen, C.Q., Li, P., Chen, Q.Y., 2016. Essential factors of an integrated moving bed biofilm reactor-membrane bioreactor: adhesion characteristics and microbial community of the biofilm. *Bioresour. Technol.* 211, 574–583.

Tang, K., Ooi, G.T.H., Litty, K., Sundmark, K., Kaarsholm, K.M.S., Sund, C., Kragelund, C., Christensson, M., Bester, K., Andersen, H.R., 2017b. Removal of pharmaceuticals in conventionally treated wastewater by a polishing moving bed biofilm reactor (MBBR) with intermittent feeding. *Bioresour. Technol.* 236, 77–86.

Young, B., Banihashemi, B., Forrest, D., Kennedy, K., Stintzi, A., Delatolla, R., 2016. Meso and micro-scale response of post carbon removal nitrifying MBBR biofilm across carrier type and loading. *Water Res.* 91, 235–243.

Zhang, P., Fang, F., Chen, Y.P., Shen, Y., Zhang, W., Yang, J.X., Li, C., Guo, J.S., Liu, S.Y., Huang, Y., Li, S., Gao, X., Yan, P., 2014. Composition of EPS fractions from suspended sludge and biofilm and their roles in microbial cell aggregation. *Chemosphere* 117, 59–65.

Zhou, G., Zhou, Y., Zhou, G., Lu, L., Wan, X., Shi, H., 2015. Assessment of a novel overflow-type electrochemical membrane bioreactor (EMBR) for wastewater treatment, energy recovery and membrane fouling mitigation. *Bioresour. Technol.* 196, 648–655.

Zhu, Y., Zhang, Y., Ren, H.Q., Geng, J.J., Xu, K., Huang, H., Ding, L.L., 2015. Physicochemical characteristics and microbial community evolution of biofilms during the start-up period in a moving bed biofilm reactor. *Bioresour. Technol.* 180, 345–351.